Study on the Radical Polymerization Behavior of Macromonomers†

Yasuhisa Tsukahara,* Kazuhiko Mizuno, Atsushi Segawa, and Yuya Yamashita

Department of Synthetic Chemistry, Faculty of Engineering Nagoya University, Nagoya 464, Japan. *Received June 28, 1988*

ABSTRACT: A study on the radical polymerization behaviors of styrene macromonomer (end group is methacrylate, M_n = 12 400, M_w/M_n = 1.06, f = 0.86) and on the characterization of produced poly(macromonomer)s was performed to clarify the characteristic feature of macromonomer polymerization systems. Polymerizations were carried out with AIBN in benzene at 60 °C. Degrees of polymerization (D_p) and the mean square radii of gyration ($\langle S^2 \rangle_b$) of produced poly(macromonomer)s and the polymerization rate (R_p) were determined by gel permeation chromatography combined with a laser light scattering detector. It was found that the D_p's of poly(macromonomer)s strongly depended upon the macromonomer concentration in feed ([M]) due to the gel effect; however, in contrast to the small monomer, D_p is not dependent much upon the conversion. The ratio of $\langle S^2 \rangle_b$ to that of the linear polystyrene of the same molecular weight, g, was also evaluated. It was found that g values at large D_p were considerably small and that the dependence of g upon D_p had almost the same tendency predicted for the star-shaped polymer in the molecular weight range of less than 1×10^6. This indicates that the propagating poly(macromonomer) radicals are very compact, and consequently, the segment density around the propagating radical site is very large. The kinetic order of [M] in the polymerization equation of R_p versus [M] was found to be about 2, and it tended to further increase at higher [M] due to the strong gel effect. The kinetic order of the initiator concentration ([I]) was found to be nearly 0.5 at low [M], whereas the order decreased at high [M] where poly(macromonomer)s of large D_p were produced. This fact indicated that the bimolecular termination did become more difficult as a consequence of the high segment density around the propagating radical sites.

Introduction

Recently, the number of studies on the synthesis and application of macromonomers has rapidly increased because of recognition of its important synthetic route to various kinds of functional graft copolymers.[1-11] However, polymerization as well as copolymerization behaviors of macromonomers are not well understood at present.[12-16] Furthermore, the true molecular weights of produced poly(macromonomer)s have been scarcely measured, and instead, the apparent molecular weights correlated with linear polystyrene standards have often been used, so the maximum degree of polymerization is still under discussion in terms of the segment density of poly(macromonomer) radicals. In comparison with polymerization systems of small monomers, the polymerization system of macromonomers may be characterized by the following features: (i) high viscosity of the polymerization media from the beginning of the polymerization, (ii) low concentration of the polymerizable reactive end group, (iii) the propagating step is a repeat of the polymer–polymer reaction, and (iv) high segment density or multibranched structure around the propagating radical site. These features suggest that the polymerization of macromonomers might be unusually sensitive to the diffusion-controlled step of polymerization reaction.[18-28] The segment density or the chain dimension of poly(macromonomer) radicals must differ markedly from those of linear polymer radicals, and it is of interest to discover how those features influence the maximum attainable degree of polymerization and the polymerization kinetics of macromonomers. Furthermore, in the case of the polymerization of high molecular weight macromonomers, the segmental diffusion of the reactive sites might become reptative and is affected by entanglements formation as the macromonomer concentration increases.[29-32] In that case, the highly multibranched structure of the poly(macromonomer) propagating radicals might be unfavorable to move through the entangled polymer system, which can also influence the polymerization kinetics. Therefore, it is very interesting and worthwhile to investigate the polymerization behavior of macromonomers to know how the diffusion-controlled step influences the chemically controlled nature of the polymerization reaction in general.

Scheme I

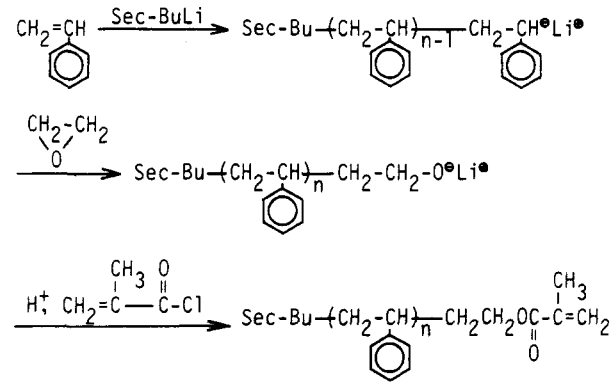

For this purpose, we investigated the homopolymerization behavior of the macromonomer using a particular monodispersed styrene macromonomer having a MMA end group in homogeneous solutions to evaluate the following points: (i) molecular weights of the produced poly(macromonomer)s and their dependence upon macromonomer concentration in the feed, (ii) segment density and radius of gyration of poly(macromonomer) radicals, and (iii) kinetic order or exponent of the polymerization equation. Gel permeation chromatography (GPC) combined with a laser light scattering detector was fully used to evaluate these points. This work may provide useful information not only for understanding the characteristic features of the polymerization system of macromonomers but also for understanding the diffusion-controlled process widely observed in polymerization of conventional small monomers.

† Presented at the 37th Annual Meeting of the Society of Polymer Science, Nagoya, Japan, May 26, 1988.

0024-9297/89/2222-1546$01.50/0

Experimental Section

Materials. The styrene (St) macromonomer having a methacrylate end group used in this study was prepared by the method employed by Milkovich,[14,16] which is shown in Scheme I. St, ethylene oxide, methacryloyl chloride, azobis(isobutyronitrile) (AIBN), and solvents are commercially available. Solvents were dried and distilled under nitrogen atmosphere. AIBN was purified by recrystallization with methanol. Styrene, ethylene oxide, methacryloyl chloride, and benzene used to prepare the macromonomer by the living anion polymerization were dried and purified under high vacuum in the usual way. *sec*-BuLi was prepared from the reaction of *sec*-butyl chloride with Li metal in *n*-hexane. The weight-average molecular weight of the macromonomer is 13 100, and the polydispersity index is M_w/M_n = 1.06. The end functionality, f, estimated with ^{1}H NMR and IR, is 0.86.

Polymerization of Macromonomer. Polymerization of the St macromonomer was carried out in benzene (or cyclohexane) solution with AIBN as an initiator at 60 °C. The macromonomer concentration in the feed, [M], was varied from 7.1×10^{-3} to 6.0×10^{-1} (mol/L), and the concentration of AIBN in the feed, [I], was varied from 3.5×10^{-3} to 3.7×10^{-2} (mol/L). The mixture of the macromonomer, solvent, and initiator was equally divided into seven or eight parts and placed in glass ampules. Each ampule was degassed, sealed, and placed in the thermostate bath controlled at 60 °C, and polymerizations were done at various polymerization times. Then, the ampule was cooled to −78 °C, and the polymerization product was taken out and freeze-dried with benzene.

Evaluation of Molecular Weight, Radius of Gyration, and Polymerization Rate. The molecular weights (M_w) and the radius of gyration ($\langle S^2 \rangle$) of the obtained poly(macromonomer)s as well as the polymerization rate (R_p) of the macromonomer were determined by using GPC. GPC measurements were carried out with a high-speed liquid chromatograph, HLC-802A of Tosoh (Toyo Soda) Co. Ltd., equipped with a low-angle laser light scattering detector, LS-8 (He–Ne laser with detection angle of 5°), in addition to the conventional RI and UV detectors, which was operated with Tosoh G6000H-G4000H-G2000H columns at 25 °C on toluene (solvent flow rate was 1.2 mL/min). Degrees of conversion were determined by the change in the ratio of the peak area of the unreacted macromonomer to the total peak area of the polymerization product in GPC charts with consideration of the end group functionality. The concentration of the sample injected was kept small, typically less than 0.1 wt % (1×10^{-8} mol/L), to minimize the concentration effect in the detected scattering light intensity.

Results and Discussion

Molecular Weights of Produced Poly(macromonomer)s. Molecular weights of the produced poly(macromonomer)s were measured to elucidate the relation between the degree of polymerization and the polymerization conditions. Combination of GPC with a low-angle light scattering (LS) detector is very useful to measure the molecular weight of branched polymers such as poly(macromonomer)s, since one can measure the true molecular weight of produced poly(macromonomer)s very fast and does not need any isolation procedures to remove unreacted macromonomers.

Typical chromatograms of poly(macromonomer)s of different molecular weights taken with LS and RI detectors are shown in Figure 1. When the concentration of solute C is very small and the scattering angle of detection is low, the Rayleigh ratio is given by the product of the molecular weight and the concentration of the solute. Under this condition, the weight-average molecular weight (M_w) of poly(macromonomer)s can be calculated from the peak area ratio of LS and Ri detectors as follows:[34]

$$M_w = (k_1/k_2K)(A^{LS}/A^{RI}) \quad (1)$$

where A^{LS} and A^{RI} are the peak area of poly(macromonomer)s taken with LS and RI detectors, respectively. The

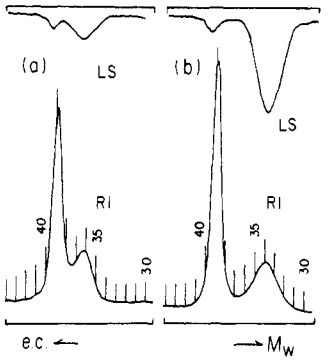

Figure 1. Typical GPC charts of the polymerization products taken by LS and RI detectors. The right peak in each chart corresponds to the produced poly(macromonomer), and the left peak corresponds to the unreacted macromonomer. M_w's of the poly(macromonomer)s are (a) 4.09×10^4, no. 6 of Table I; (b) 36.2×10^4, no. 12 of Table I (toluene; 25 °C; flow rate, 1.2 mL/min; 1 elution count is equal to 1 mL).

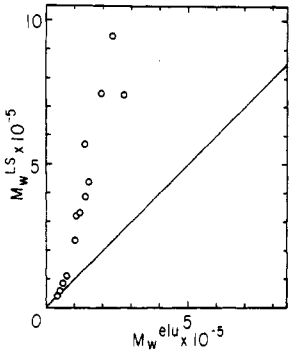

Figure 2. True molecular weight determined using LS response curve versus the apparent one determined using molecular weight–elution volume calibration curves of linear polystyrene standards.

constants, k_1, k_2, and K are the proportionality constants defined by

$$h_i^{RI} = k_1 C_i$$

$$h_i^{LS} = k_2 R_\theta = k_2 K C_i M_i \quad (2)$$

where h_i^{RI} and h_i^{LS} are the response intensities at elution volume i detected by RI and LS, respectively. M_i and C_i are the molecular weight and the concentration of the solute corresponding to the elution volume i, and R_θ is the Rayleigh ratio. Then, M_w/M_n can be calculated by eq 1 and 3. The product k_1/k_2K, the instrument constant, was

$$M_n = \sum_i h_i^{RI} / \sum_i (h_i^{RI}/M_i) \quad (3)$$

determined with linear polystyrene standards with different molecular weights, and the average value was around 2×10^5 with toluene at 25 °C. This value was independent of the molecular weight of the standard polystyrene samples but dependent of optical conditions.

In Figure 2, the molecular weights of poly(macromonomer)s (M_w^{LS}) thus obtained were plotted against the apparent molecular weight (M_w^{elu}), which was determined from the elution volume correlating with the linear polystyrene standards. The molecular weights of poly(macromonomer)s with various polymerization conditions are also summarized in Table I. It is clearly seen from Figure 2 that the molecular weights of the poly(macromonomer)s determined with the LS detector become appreciably larger than the apparent values as D_p increases. M_w^{LS} reaches 1×10^6 as the apparent value reaches about 2.5×10^5. In other words, the more the degree of polymerization increases, the more the poly(macromonomer) be-

Table I
Molecular Weight of Poly(macromonomer)s and Polymerization Conditions

no.	feed concn, 10^{-2} mol/L [M]	feed concn, 10^{-2} mol/L [I]	polymz. time, h	10^4M_w[a]	M_w/M_n	D_p	10^4M_w app[b]
1	0.71	0.35	48	3.5	1.20	2.7	3.5
2	0.85	1.79	48	4.3	1.10	3.3	4.2
3	1.26	0.79	48	11.1	1.16	8.5	7.4
4	1.60	1.64	48	3.6	1.21	2.8	3.6
5	2.19	1.64	48	7.5		5.7	
6	2.20	1.64	24	4.1	1.48	3.1	3.9
7	2.81	1.50	8.5	6.0	1.31	4.6	5.0
8	2.81	1.50	48	23.8		18.2	
9[c]	2.81	1.50	48	32.1	2.93	24.5	10.8
10	2.83	2.00	48	15.5		11.8	
11	2.84	1.64	48	38.7	5.64	29.5	14.0
12	2.85	1.82	24	36.2	2.72	27.6	11.4
13	2.89	1.50	48	33.2	1.62	25.3	11.8
14	3.16	2.00	48	20.0		15.3	
15	3.38	2.00	48	22.3		17.0	
16	3.60	1.64	48	43.7	1.97	33.4	15.1
17	3.85	3.71	48	48.4		36.9	
18	3.89	1.50	1	94.5	2.81	72.1	23.4
19	3.89	1.50	2.5	74.6	3.20	56.9	19.4
20	3.89	1.50	8.5	74.0	2.25	56.5	27.5
21	3.89	1.50	24	56.8	1.59	43.4	13.7
22[d]	6.00	1.50	48	543.0	1.72	414.5	132.0

[a] Determined from eq 1. [b] Determined from molecular weight–elution volume calibration curve of linear polystyrene standards. [c] Polymerization was carried out in cyclohexane. [d] Macromonomer/benzene/AIBN mixture was prepared from freeze-drying method because the viscosity of the mixture was very high and the concentration was roughly estimated from the weight change during the freeze-drying procedure.

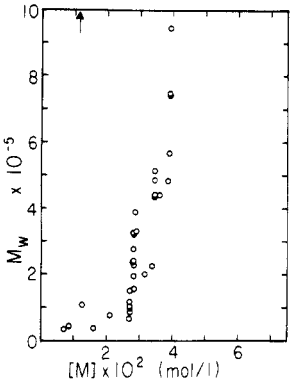

Figure 3. Variation of the weight-average molecular weight (M_w) of poly(macromonomer)s with the feed concentration of macromonomer, [M]. Polymerizations were carried out in benzene at 60 °C. The arrow in the figure corresponds to the overlap concentration (C^*) of the linear polystyrene of the same molecular weight as the macromonomer.

comes compact compared with a linear polymer. Thus, the apparent values often used for convenience are appreciably smaller than the true values.

The M_w's of the poly(macromonomer)s determined with the LS detector were plotted against the feed macromonomer concentration, [M], in Figure 3. It can be seen from the figure that M_w is very small (D_p = 3–5) at [M] less than ca. 2×10^{-2} mol/L. Beyond this concentration, the molecular weight rapidly increases to a great extent with an increase of [M]. However, the M_w (or D_p) of poly(macromonomer) is not very dependent on the reaction time or the degree of conversion, as shown in Figure 4. Rather, a decreasing tendency can be seen in Table I (no. 18–21), probably because the concentration of unreacted macromonomer and initiator decrease with an increase of the

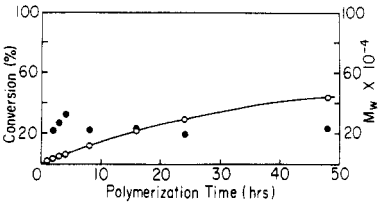

Figure 4. Degrees of conversion (○) and weight-average molecular weight (●) plotted against polymerization time. Polymerizations were carried out with [M] = 2.81×10^{-2} mol/L and [I] = 1.50×10^{-2} mol/L in benzene at 60 °C.

Table II
Effect of Initiator Concentration on M_w[a]

no.	[I], 10^{-2} mol/L	polymz. time, h	$10^{-4}M_w$
1	0.420	6	14.9
2	0.609	6.5	10.2
3	0.755	6	11.6
4	1.04	6	7.5
5	1.10	6.5	8.5
6	1.38	6	8.9
7	1.91	6	6.6
8	2.56	6.5	9.5

[a] Polymerizations were carried out in benzene at 60 °C with [M] = 2.70×10^{-2} mol/L.

degree of conversion. This molecular weight–degree of conversion relationship in the macromonomer system is quite different from that in the small monomer system, whereby the large increase of the molecular weight is normally observed with an increase in the degree of conversion at high monomer concentration due to the gel effect (autoacceleration effect or Trommsdorf effect).[19,21,25]

These results can be reasonably interpreted by the characteristic features in the polymerization system of macromonomers. In contrast to the polymerization system of small monomers, the gel effect does appear from the beginning of polymerization reaction in the macromonomer system because of the high viscosity of the polymerization media due to the presence of macromolecular monomers. Hence, the extent of the gel effect is basically a function of the amount of existing macromonomer in the feed. However, judging from the molecular weight versus conversion relationship in Figure 4, the effect seems to be almost independent of the proceeding of polymerization. The effect of the initiator concentration on M_w is shown in Table II, where no large effect or a slight decreasing tendency with [I] can be seen. The extent of the observed gel effect in Figure 3 markedly increases above [M] = ca. 0.03 mol/L, whereas below this concentration the effect is small. The overlap concentration (C^*) of the macromonomer solution with M_w = 13 100 is 1.1×10^{-2} mol/L, in which the difference between benzene and toluene and temperature effect was neglected.[40] Thus, the large increase of the gel effect appears to be about 3 times larger than C^* above the concentration.

Furthermore, the fact that the degree of polymerization of poly(macromonomer) can reach almost 70 at [M] = 0.04 mol/L indicates that the high peripheral segment density of the radical site associated with the multibranched structure of the propagating chain does not further hinder incorporation of macromonomers, at least in the range of D_p less than 70 (corresponding M_w is ca. 1×10^6). It should be noted that the polydispersity indexes (M_w/M_n) of the poly(macromonomer)s were relatively small, especially those obtained with small [M] (no. 11 in Table I is the only exception).

Segment Density and Radius of Gyration of Poly(macromonomer) Radicals. Further, we intended to

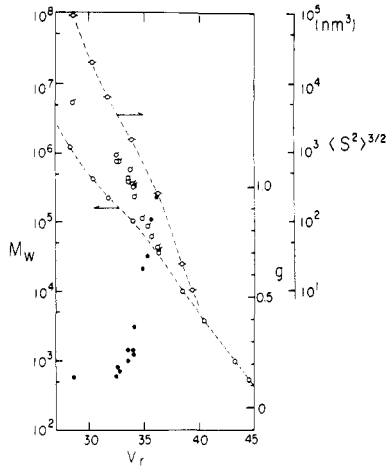

Figure 5. Plots of $\langle S^2\rangle^{3/2}$ of poly(macromonomer)s versus V_r (-O-), M_w of poly(macromonomer)s (Ø) and linear polystyrene standards (O) versus V_r, and g versus V_r (●) in toluene at 25 °C. Flow rate was 1.2 mL/min, and 1 elution count is equal to 1 mL.

Table III
Radius of Gyration and Segment Density of Poly(macromonomer)s

no.	$10^{-4}M_w$	$\langle S^2\rangle_b^{1/2}$, nm	g	C^*,[a] 10^{-2} g/mL	segment density,[b] St units/nm^3 PM[c]	segment density,[b] St units/nm^3 linear[d]
2	4.28	6.52	0.949	6.13	0.355	0.327
7	6.02	7.56	0.850	5.53	0.320	0.251
e	8.55	8.34	0.681	5.84	0.338	0.191
3	11.1	9.36	0.626	5.37	0.311	0.153
e	23.5	11.1	0.364	6.75	0.391	0.085 6
9	32.1	11.4	0.262	8.66	0.501	0.067 6
13	33.2	11.0	0.238	9.83	0.569	0.065 7
11	38.7	12.6	0.259	7.67	0.444	0.058 1
16	43.7	12.6	0.224	8.62	0.499	0.052 8
21	56.8	11.8	0.144	13.6	0.785	0.043 0
20	74.0	15.6	0.183	7.72	0.447	0.035 0
19	74.6	14.9	0.165	9.02	0.522	0.034 9
18	94.5	15.8	0.140	9.55	0.553	0.028 9
22	543.0	45.1	0.143	2.33	0.135	0.007 29

[a] Overlap concentration calculated from $C^* = 3M_w/(4\pi\langle S^2\rangle^{3/2}N_A)$. [b] Calculated from $\rho_s = C^*N^A/M_{St}$, where M_{St} is molecular weight of a styrene monomer unit. [c] Poly(macromonomer). [d] Linear polystyrene of the same molecular weight as the poly(macromonomer). [e] These are not listed in Table I because the feed concentrations are uncertain.

evaluate the segment density of the poly(macromonomer)s with GPC to understand how the high peripheral segment density of the propagating radical influences D_p and the polymerization kinetics of the macromonomer. The mean square radius of gyration of poly(macromonomer)s, $\langle S^2\rangle_b$, can be estimated from a GPC chromatograph, with the $\langle S^2\rangle$ versus elution volume (V_r) calibration curve.[34,42] To construct this calibration curve, the conventional M_w versus V_r calibration curve of linear polystyrene standards for GPC was combined with the following empirical equation for the radius of gyration versus molecular weight relationship for linear polystyrenes in toluene 25 °C,[34] assuming that the calibration curve is valid for both linear and branched polymers:

$$\langle S^2\rangle_l = 1.38 \times 10^{-18}M_w^{1.19} \quad (4)$$

The $\langle S^2\rangle^{3/2}$ versus V_r relationship thus obtained is shown in Figure 5 together with M_w versus V_r plots. $\langle S^2\rangle^{3/2}$ values of poly(macromonomer)s are summarized in Table III together with M_w. The relationship between the effective (hydrodynamic) volume of the separation processes in GPC and the static radius of gyration measured by a light scattering technique for a branched polymer is not exactly equal to that for the linear polymers,[37,38] so direct measurement of $\langle S^2\rangle_b$ by such a small-angle X-ray scattering measurement of these poly(macromonomer)s might be necessary to discuss the segment density of poly(macromonomer) radicals quantitatively.[35] However, from these values, we can draw some specific features of the propagating radicals during the polymerization.

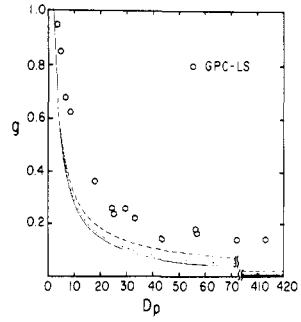

Figure 6. g values versus degrees of polymerization of poly(macromonomer)s. Open circles are experimental values evaluated from eq 5. Solid curve, dotted curve, and broken curve are theoretical ones, each of which was calculated from eq 7 and 8 with $z = 0.1$ and 0.5, respectively.

g values defined by the ratio of the mean square radius of gyration of poly(macromonomer) to that of the linear polymer of the same molecular weight were also evaluated

$$g = \langle S^2\rangle_b/\langle S^2\rangle_l \quad (5)$$

where $\langle S^2\rangle_l$ values were determined from eq 4 using M_w^{LS} of the poly(macromonomer). The g values thus evaluated are given in Table III and plotted against V_r in Figure 5. The dependence of g on D_p is shown in Figure 6. In this work, D_p corresponds to the ratio of M_w of the poly(macromonomer) to that of the macromonomer and equals the number of branch units, f.

The g value can also be calculated theoretically. Under the Θ condition, for the comb-shaped polymer, g is given by [39,40]

$$g = (1 + f\gamma)^{-3}[1 + 2f\gamma + (2f + f^2)\gamma^2 + (3f^2 - 2f)\gamma^3] \quad (6)$$

where γ is the ratio of the molecular weight of a branch to that of the backbone. g for the star-shaped polymer is given by

$$g = (3f - 2)/f^2 \quad (7)$$

When the excluded volume effect exists, g value for the star-shaped branched polymer near Θ temperature is given by[41]

$$g = [(3f - 2)/f^2][(1 + K_bZ + ...)/(1 + 1.276Z + ...)] \quad (8)$$

where Z is the excluded volume parameter and K_b is given by

$$K_b = \frac{3}{[(f^{0.5}(3f - 2)]}\left[\frac{67(2^{7/2})}{315}(f - 1) - \frac{134}{315}(f - 2) + \frac{4}{45}(11(2^{0.5}) - 138)(f - 1)(f - 2)\right] \quad (9)$$

In this work, γ in eq 6 equals $126/D_p$. The calculated curve of g versus f from eq 6 was almost identical with the curve from eq 7 at D_p less than 70, indicating that poly(macromonomer)s prepared from the macromonomer of this

molecular weight can be considered as nearly star-shaped polymers. The theoretical curves from eq 7 (solid curve) and from eq 8 with $Z = 0.1$ (dotted curve) and $Z = 0.5$ (broken curve) are shown in Figure 6. It is seen from the calculated curves in Figure 6 that, from a theoretical point of view, the g value increases with an increase in the excluded volume effect. That is, the decrease in the molecular dimension due to branching is compensated in part by the excluded volume effect. The experimental g value variation with D_p in Figure 6 has an almost identical tendency but rather higher than the calculated value. This is quite reasonable since the experimental g values were evaluated in a good solvent (toluene at 25 °C), where a large excluded volume effect can be expected. This can expand the poly(macromonomer) chains to a larger extent compared to the linear polymer because of the higher segment density or the greater chance of segment contact. g variation with D_p in Figure 6 provides evidence that there is no or negligible formation of irregularly shaped poly(macromonomer)s by such chain-transfer reactions to polymer during polymerization.

Poly(macromonomer) having D_p =414 is the only exception. The g value of this poly(macromonomer) at V_r = 28.62 in Figure 5 is considerably larger than the expected value from the extrapolation of other data at large V_r and almost the same as those of poly(macromonomer)s at V_r = 32.5–33.0. In Figure 6, the g value of this poly(macromonomer) is also considerably larger than the calculated one. A partial reason for this might be ascribed to the formation of an irregularly shaped poly(macromonomer), although the reason of irregularity is not clear at present. Another reason may come from its high D_p, because poly(macromonomer)s having such high D_p are not star shaped but rather comb-type branched polymers (the length of the backbone segment is about 4 times that of branch segments). It should be noted that the polymerizable end group of the macromonomer is methacrylate, and thus this part of the poly(styrene macromonomer)s can also influence the chain dimension of the poly(macromonomer). This effect might increase as D_p (backbone length) increases or as M_w of the macromonomer decreases.

In Table III, the value of the segment density (ρ_s) of poly(macromonomer)s, the number of styrene monomer units per cubic nanometer, calculated from eq 10 is shown

$$\rho_s = 3M_w/(4\pi\langle S^2\rangle^{3/2}M_{St}) = C^*/N_AM_{St} \quad (10)$$

together with those of the corresponding linear polystyrene where M_{St} is the molecular weight of the styrene monomer unit. It is seen in Table III that ρ_s of poly(macromonomer) is a slow, increasing function of M_w, whereas ρ_s of linear polystyrene decreases very rapidly with an increase in M_w. In turn, the segment density of poly(macromonomer)s of high M_w is much higher than those of linear polystyrene. Further, in the case of the propagating poly(macromonomer) radicals, the radical site is located at the center of the multibranched structure, so that the local segment density around the radical site must be much higher than the overall value (ρ_s) in Table III. The detailed segment density around the propagating radicals is being measured at present and will be discussed in the following paper.

Kinetic Order of Polymerization. In this section, we focused on the dependence of the radical polymerization (R_p) of macromonomer on the feed macromonomer concentration, [M], the initiator concentration, [I], and the change of kinetic order in our macromonomer system from those in the polymerization system of a small monomer in dilute solution, where R_p is given by[44]

$$R_p = k_p(2fk_d/k_t)^{1/2}[M][I]^{1/2} \quad (11)$$

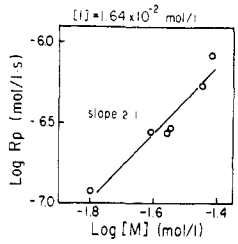

Figure 7. Double-logarithmic plot of polymerization rate (R_p) versus feed concentration of macromonomer ([M]). Polymerizations were carried out with [I] = 1.64×10^{-2} mol/L in benzene at 60 °C.

where k_p, k_t, and k_d are the rate coefficients of propagation, termination, and initiator decomposition, respectively. f is the initiator efficiency.

In Figure 7, R_p variations with [M] at fixed [I] = 1.62×10^{-2} mol/L are shown. It is seen in Figure 7 that R_p depends on [M], with higher than first order. The obtained apparent order is 2.1 in the range from [M] = 1.5×10^{-2} to 4.0×10^{-2} mol/L; however, the value seems to become greater as [M] increases further. The deviation from first order with respect to [M] can be attributed to the high viscosity of polymerization media due to the presence of macromolecular monomer. The high viscosity increases $k_p/(2k_t)^{1/2}$ due to the diffusion-controlled termination. This gel effect as a function of [M] was already seen in the M_w versus [M] relationship shown in Figure 3.

In the case of the polymerization system of macromonomers, however, the propagation reaction is the repeat of polymer–polymer reaction, where the rearrangement of both the propagating chain and the macromonomer chain by segmental diffusion is required in each propagation step to allow the close approach of the radical sites and the polymerizable end groups. Therefore, the propagating rate constant (k_p) can be influenced by the segment density around the propagating radical sites.

Further, in this study, the macromonomer concentration in feed ranges from 7.1×10^{-3} to 6.0×10^{-1} mol/L, which covers above the overlap concentration of this macromonomer. Therefore, in addition to the segment density, the decrease of the segmental diffusivity associated with the specific multibranched structure of poly(macromonomer) radicals should also be taken into account at higher concentration above C^*. The effect of the decrease in diffusivity of multibranched polymer species on k_t might be much larger above the critical concentration for the entanglement formation, since diffusion of the polymer reaction species in the polymerization media becomes reptative at such high feed concentration. Consequently, approach of the radical site and the polymerizable end group becomes more difficult as the number of branches increases due to the topological resistance from the polymerization media.[33] However, the entanglement threshold of bulk polystyrene is around $M_w = 3 \times 10^4$–4×10^4 [25,29,32] and increases with dilution. The maximum contour length of the poly(macromonomer) radicals here is less than $M_w = 3 \times 10^4$, so the poly(macromonomer) radicals in this work are not long enough to be entangled in spite of their large molecular weights. Thus, the entanglement effect can be considered to be small during the polymerization of this macromonomer.

From the experimental fact that the large increases of R_p and M_w with [M] were observed in this macromonomer system, it is seen that the decrease of k_p with increase in [M] is not discernible and minor compared with the decrease of k_t.

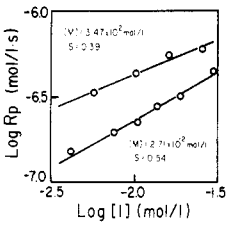

Figure 8. Double-logarithmic plot of polymerization rate (R_p) versus initiator concentration. Polymerizations were carried out with [M] = 2.71×10^{-2} and 3.47×10^{-2} mol/L in benzene at 60 °C.

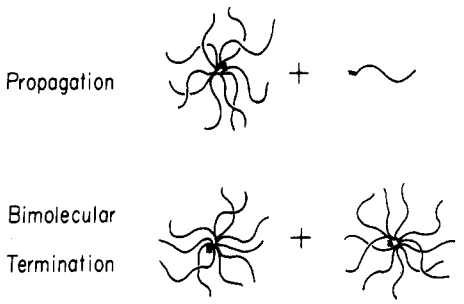

Figure 9. Schematic representation of the propagation reaction and the bimolecular termination reaction in the macromonomer polymerization system.

The increase in viscosity may also have an influence on the initiator efficient (f) in eq 11. f becomes dependent on [M] at high [M] due to the decreased mobility of the primary radicals (the cage effect).[44,45] This also cause a R_p variation with [M] to some power. Therefore, it is seen that the observed apparent kinetic order of [M] involves these factors.

In Figure 8, R_p variations with [I] at particular macromonomer concentrations of [M] = 2.71×10^{-2} and 3.47×10^{-2} mol/L are shown. It is seen from Figure 8 that R_p depends on [I] with almost half order at lower [M], whereas at higher [M] the dependence of R_p upon [I] is less than half order. This result can be explained as follows. That is, at [M] = 2.71×10^{-2} mol/L, the D_p of the produced poly(macromonomer) is estimated to be about 10–20 from Figure 3, and the g value is not small, so the bimolecular termination of poly(macromonomer) radicals takes place with little difficulty. However, at [M] = 3.47×10^{-2} mol/L, where D_p expected from Figure 3 is about 40 (corresponding g in Figure 6 is about 0.2), the bimolecular termination becomes more difficult, since the higher peripheral segment density of the propagating radicals may sterically hinder the bimolecular termination, as shown in Figure 9. This causes the competing primary radical termination reaction to be more important. Such hindrance of the bimolecular termination is presumably more remarkable at much higher [M] like bulk condition. However, the increase in viscosity of the polymerization media with an increase of [M] can also enhance the cage effect, which increases the recombination of the geminate primary radicals and consequently suppresses the primary radical termination effect.

Furthermore, at very large [M] region, the local polymer structure around the propagating radical sites should also be taken into account, since the large molecular weight poly(macromonomer)s are formed at high [M]. Such large molecular weight poly(macromonomer)s cannot be considered as nearly star-shaped polymers but rather as comb-type branched polymer as previously mentioned, where the local steric hindrance around the radical site for the bimolecular termination is much smaller than that expected for the star-shaped polymer. The peripheral segment density around the radical site may presumably saturate at large D_p.

It should be noted that the macromonomer in this work cannot be polymerized under bulk condition (without solvent), since the polymerization temperature is below the glass transition temperature of this styrene macromonomer. Therefore, there must be a certain [M] which gives the maximum D_p and R_p. Above this concentration, D_p and R_p might presumably decrease again with [M]. Consequently, the observed kinetic order of [I] at large [M] is governed by the balance of these factors. Further study on the polymerization behavior at higher [M] with different molecular weight macromonomers including the direct measurement of the molecular dimension and the segment density around the propagating radicals is now in progress and will appear elsewhere.

Acknowledgment. We are indebted to Prof. I. Noda of Nagoya University and Prof. T. Kato of Mie University for their valuable discussions. This research was supported in part by a Grant-in-Aid for Scientific Research from Ministry of Education, Science and Culture, Japan (No. 63750866).

References and Notes

(1) Yamashita, Y. *J. Appl. Polym. Sci., Appl. Polym. Symp.* **1981**, *36*, 193.
(2) Tsukahara, Y.; Tsai, H.-C.; Yamashita, Y.; Muroga, Y. *Polym. J.* **1987**, *19*, 1033.
(3) Tsukahara, Y.; Kohno, K.; Inoue, H.; Yamashita, Y. *Nippon Kagaku Kaishi* **1985**, *6*, 1070.
(4) Tsukahara, Y.; Kohno, K.; Yamashita, Y. In *Current Topics in Polymer Science*; Ottenbrite, R. M.; Utracki, L. A., Inoue, S., Eds.; Hanser Publisher: Munich–Vienna–New York, 1987; Vol. II, p 333.
(5) Yamashita, Y.; Tsukahara, Y. In *Modification of Polymers*; Carraher, C., Moore, J., Eds.; Plenum Press: New York, 1983; pp 131–140.
(6) Kawakami, Y.; Miki, Y.; Tsuda, T.; Murthy, R. A. N.; Yamashita, Y. *Polym. J.* **1982**, *14*, 913.
(7) Chujo, Y.; Shishino, T.; Tsukahara, Y.; Yamashita, Y. *Polym. J.* **1985**, *17*, 133.
(8) Ito, K.; Usami, N.; Yamashita, Y. *Macromolecules* **1980**, *13*, 216.
(9) Asami, R.; Takaki, M.; Kita, K.; Asakura, E. *Polym. Bull.* **1979**, *2*, 713. Asami, R.; Takaki, M.; Kyuda, K.; Sukenaga, N. *Polym. J.* **1983**, *15*, 261. Takaki, M.; Asami, R.; Tanaka, S.; Hayashi, H.; Hogen-Esch, T. *Macromolecules* **1986**, *12*, 2900.
(10) Nishimura, T.; Maeda, M.; Nitadori, Y.; Tsuruta, T. *Macromol. Chem. Rapid. Commun.* **1979**, *180*, 1877. Nagasaki, Y.; Tsuruta, T. *Makromol. Chem.* **1986**, *187*, 1583.
(11) Rempp, P. F.; Franta, E. *Adv. Polym. Sci.* **1984**, *58*, 1. Sierra-Vagas, J.; Franta, E.; Rempp, P. F. *Makromol. Chem.* **1981**, *182*, 2603.
(12) Ito, K.; Tsuchida, H.; Hayashi, A.; Kitano, T.; Yamada, E.; Matsumoto, T. *Polym. J.* **1985**, *15*, 827.
(13) Cameron, G. G.; Chisholm, M. S. *Polymer* **1985**, *26*, 437; **1986**, *27*, 1420.
(14) Schulz, G. O.; Milkovich, R. *J. Polym. Sci., Polym. Chem. Ed.* **1984**, *22*, 1633.
(15) Kennedy, J. P.; Lo, C. Y. *Polym. Bull.* **1982**, *8*, 63; **1985**, *13*, 343.
(16) Tsukahara, Y.; Tanaka, M.; Yamashita, Y. *Polym. J.* **1987**, *19*, 1121.
(17) Tsukahara, Y.; Hayashi, H.; Jiang, X.-L.; Yamashita, Y., submitted for publication in *Polym. J.*
(18) Smoluchowski, M. *Z. Phys. Chem.* **1918**, *92*, 129.
(19) Trommsdorf, E.; Kohle, H.; Lagally, P. *Makromol. Chem.* **1948**, *1*, 169.
(20) de Gennes, P.-G. *J. Chem. Phys.* **1982**, *76*, 3316, 3322.
(21) Tulig, T.; Tirrell, M. *Macromolecules* **1981**, *14*, 1501.
(22) Cameron, G. G.; Cameron, J. *Polymer* **1973**, *14*, 107.
(23) Morawetz, H.; Cho, J. R.; Gans, P. J. *Macromolecules* **1973**, *6*, 624.
(24) Horie, K.; Mita, I.; Kambe, H. *Polym. J.* **1973**, *4*, 341. Horie, K.; Mita, I. *Macromolecules* **1978**, *11*, 1175.
(25) Mita, I.; Horie, K. *J. Macromol. Sci.-Rev. Macromol. Chem. Phys.* **1987**, *C27*, 91–169.
(26) O'Driscoll, K. F.; Mahabadi, J. *J. Polym. Sci., Polym. Chem., Ed.* **1976**, *14*, 869. O'Driscoll, K. F. *Ibid.* **1977**, *15*, 283.

(27) Iwata, H.; Ikada, Y. *Makromol. Chem.* **1980**, *181*, 517.
(28) Turner, D. T. *Macromolecules* **1977**, *10*, 221, 226, 231.
(29) Onogi, S.; Masuda, T.; Kitagawa, K. *Macromolecules* **1970**, *3*, 107.
(30) Graessley, W. W. *Adv. Polym. Sci.* **1974**, *16*, 1.
(31) Tirrell, M. *Rubber Chem. Technol.* **1984**, *57*, 523.
(32) Takahashi, Y.; Noda, I.; Nagasawa, M. *Macromolecules* **1985**, *18*, 2220.
(33) de Gennes, P.-G. *Scaling Concepts in Polymer Physics*; Cornell University Press: Ithaca, NY, 1979.
(34) Kato, T.; Kanda, A.; Takahashi, A.; Noda, I.; Maki, S.; Nagasawa, M. *Polym. J.* **1979**, *11*, 575. Kato, T.; Tokuya, T.; Nozaki, T.; Takahashi, A. *Polymer* **1984**, *25*, 218.
(35) This assumption means that the ratio of intrinsic viscosity of poly(macromonomer)s to that of linear polystyrene standards, $[\eta]_b/[\eta]_l$, is equal to $g^{3/2}$, since the universality of the $\langle S^2\rangle^{3/2}$ versus V_r calibration curve as well as the $[\eta]M_w$ versus V_r calibration curve is accepted for both linear and branched polymers. However, this might not be admitted when $[\eta]_b/[\eta]_l$ is equal to $g^{1/2}$. In that case, independent measurement of $\langle S^2\rangle_b^{3/2}$ is necessary to evaluate the segment density quantitatively. Combination of a multichannel light scattering photodetector with GPC is also very useful for this purpose.
(36) Noda, I.; Higo, Y.; Ueno, T.; Fujimoto, T. *Macromolecules* **1984**, *17*, 1055.
(37) Casassa, E. F.; Tagami, Y. *Macromolecules* **1969**, *2*, 14.
(38) Kurata, M.; Abe, M.; Iwama, M.; Matsushima, M. *Polym. J.* **1972**, *3*, 729, 739.
(39) Berry, G. C. *J. Polym. Sci., A-2* **1968**, *6*, 1551.
(40) Noda, I.; Horikawa, T.; Kato, T.; Fujimoto, T.; Nagasawa, M. *Macromolecules* **1970**, *3*, 795.
(41) Yamakawa, H. *Modern theory of Polymer Solutions*; Harper and Row: New York, 1971.
(42) Kato, T.; Itsubo, A.; Yamamoto, Y.; Fujimoto, T.; Nagasawa, M. *Polym. J.* **1975**, *7*, 123.
(43) Mays, J. W.; Hadjichristidis, N.; Fetters, J. L. *Macromolecules* **1985**, *18*, 2231.
(44) Odian, G. *Principles of Polymerization*, 2nd ed.; Wiley: New York, 1981.
(45) Ito, K. *Polym. J.* **1985**, *17*, 421.

Living Cationic Polymerization of Isobutyl Vinyl Ether by Hydrogen Iodide/Lewis Acid Initiating Systems: Effects of Lewis Acid Activators and Polymerization Kinetics[1]

Kazushige Kojima, Mitsuo Sawamoto, and Toshinobu Higashimura*

Department of Polymer Chemistry, Faculty of Engineering, Kyoto University, Kyoto 606, Japan. *Received April 25, 1988*

ABSTRACT: Eight initiating systems (HI/MX_n), each of which consists of hydrogen iodide and a metal halide (MX_n = ZnI_2, $ZnBr_2$, $ZnCl_2$, SnI_2, $SnCl_2$, $MgCl_2$, BF_3OEt_2, $SnCl_4$), have been employed for possible living cationic polymerization of isobutyl vinyl ether. Zinc and tin(II) halides all led to well-defined living polymerizations in toluene and in methylene chloride at −40 °C; in particular, zinc halides also permitted similar living processes in toluene even at room temperature (+25 °C). Under these conditions, the number-average molecular weights ($\bar{M}_n$) of the polymers were directly proportional to monomer conversion and inversely proportional to the initial concentration of hydrogen iodide but independent of that of MX_n. The stability of the living ends at +25 °C slightly decreased in the order $ZnI_2 > ZnBr_2 > ZnCl_2$. With $MgCl_2$, in contrast, polymerization hardly occurred under similar conditions, whereas the use of stronger Lewis acids (BF_3OEt_2 and $SnCl_4$) resulted in nonliving polymers. Kinetic studies with the HI/ZnX_2 initiating systems (X = I, Br, Cl) showed the rate of the living polymerizations to be first order with respect to monomer, hydrogen iodide, and ZnX_2 and thereby confirmed that hydrogen iodide serves as an initiator which generates the growing species and that MX_n serves as an activator which promotes its living propagation.

Introduction

Binary initiating systems (HI/I_2 and HI/ZnI_2) that consist of hydrogen iodide and a weak Lewis acid (iodine or ZnI_2) have been shown to permit well-defined living cationic polymerizations of vinyl ethers[2,4] as well as *p*-methoxystyrene.[5] The binary nature of these systems is of critical importance for attaining the living processes:[6] As visualized in Scheme I, hydrogen iodide undergoes, prior to the onset of the polymerization, quantitative electrophilic addition to the vinyl group of monomer to form an initiating adduct 1 with a carbon–iodine (C–I) bond that is per se unable to propagate. The Lewis acid component (MX_n) in turn activates the dormant C–I linkage through an electrophilic interaction so as to start the living propagation. Therefore, hydrogen iodide and the Lewis acid are termed "initiator" and "activator", respectively.[2,7]

The initiator/activator mechanism elicits two important questions: (1) What is the range of activators (MX_n) that are suited for the HI-mediated living polymerization? Namely, how do the structure and acidity of MX_n affect the living nature of the reaction? (2) What is the kinetics of the living polymerization that involves a consecutive activation of the dormant C–I terminal? This study specifically focuses on these subjects.

Scheme I

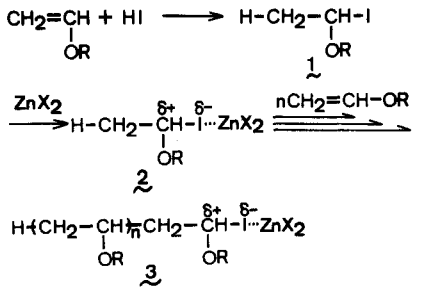

To answer the first question, we employed the following eight Lewis acids as potential activators for the living polymerization of isobutyl vinyl ether (IBVE) in the presence of hydrogen iodide: (A) ZnI_2, $ZnBr_2$, $ZnCl_2$, SnI_2, $SnCl_2$, $MgCl_2$; (B) BF_3OEt_2, $SnCl_4$. Group A consists of divalent metal halides that are relatively weak Lewis acids unable to polymerize IBVE by themselves. The two com-

0024-9297/89/2222-1552$01.50/0